Reinvestigation of high spin states and proposed octupole correlations in ^{147}Ce

H. J. Li (□□□), S. J. Zhu (□□□), J. H. Hamilton, E. H. Wang, A. V. Ramayya, Y. J. Chen (□□□), J. K. Hwang, J. Ranger, S. H. Liu, Z. G. Xiao (□□□), Y. Huang (□□), Z. Zhang (□□□), Y. X. Luo, J. O. Rasmussen, I. Y. Lee, G. M. Ter-Akopian, Yu. Ts. Oganessian, and W. C. Ma

Phys. Rev. C **90**, 047303 — Published 9 October 2014

DOI: 10.1103/PhysRevC.90.047303

Reinvestigation of high spin states and proposed octupole correlations in ^{147}Ce

H. J. Li(李红洁),[1] S. J. Zhu(朱胜江),[1,*] J. H. Hamilton,[2] E. H. Wang,[2] A. V. Ramayya,[2] Y. J. Chen(陈永静),[3] J. K. Hwang,[2] J. Ranger,[2,4] S. H. Liu,[5] Z. G. Xiao(肖志刚),[1] Y. Huang(黄彦),[1] Z. Zhang（张钊),[1] Y. X. Luo,[2,6] J. O. Rasmussen,[6] I. Y. Lee,[6] G. M. Ter-Akopian,[7] and Yu. Ts. Oganessian[7]

[1]*Department of Physics, Tsinghua University, Beijing 100084, People's Republic of China*
[2]*Department of Physics, Vanderbilt University, Nashville, Tennessee 37235 USA*
[3]*Department of Nuclear Physics, China Institute of Atomic Energy, Beijing 102413, China*
[4]*Physics Department, Furman University, Greenville, South Carolina 29613, USA*
[5]*Department of Chemistry, University of Kentucky, Lexington, Kentucky 40506, USA*
[6]*Lawrence Berkeley National Laboratory, Berkeley, California 94720 USA*
[7]*Flerov Laboratory for Nuclear Reactions, Joint Institute for Nuclear Research, 141980, Dubna, Russia*

(Dated: August 26, 2014)

High-spin states in neutron-rich ^{147}Ce have been reinvestigated by measuring the triple and four fold $\gamma-\gamma$ coincidence data observed in the spontaneous fission of ^{252}Cf. The positive-parity band is expanded to spin (45/2) $\hbar$ and the negative-parity side band has been expanded to spin (39/2) with a new third band connected to it. An octupole band structure with $s = +i$ has been proposed. The systematic characteristics of the octupole correlations have been discussed. Reflection asymmetric shell model calculations for the octupole band structure of ^{147}Ce are in good agreement with the experimental data.

PACS numbers: 21.10.Re, 23.20.Lv, 27.60.+j, 25.85.Ca

Theoretical calculations predicted the existence of octupole deformation around the $Z = 56$ and $N = 88$ neutron-rich nuclear region [1–3]. By using large detector arrays, octupole-deformed bands and octupole correlations have been identified in many nuclei in this region, especially in even-even Ba ($Z = 56$) and Ce ($Z = 58$) nuclei, such as, in ^{140,142,144,146,148}Ba [3–8], ^{144,146,148,150,152}Ce [4, 9–14]. For the odd-A nuclei in this region, octupole deformation and octupole correlations have also been identified in several nuclei, e.g. in ^{141}Cs [15], ^{143}Ba [16], ^{145,147}La [17], ^{145}Ce [18] and ^{147}Nd [18].

For the $N = 89$ odd-A isotones in this region, the octupole correlations were first identified in ^{145}Ba [16]. Then in Ref. [19], octupole-vibrational bands in this nucleus were proposed. In odd-A ^{149}Nd ($Z = 60$), several negative-parity levels were reported, and they were assigned as octupole-vibrational levels [20]. For the $N = 89$ odd-A ^{147}Ce, the level structures were reported in Refs. [21, 22], but no octupole band structure was observed. Then in Ref. [20], negative parity octupole-vibrational levels in ^{147}Ce were also reported. Search for octupole correlations in neuron-rich ^{147}Ce is valuable to systematically understand the characteristics of the nuclear structure in this region. In this paper, we report on the reinvestigation of the high-spin states in ^{147}Ce. The high-spin levels are expanded and updated, and octupole correlations are proposed. Reflection asymmetric shell model (RASM) calculations for the octupole band structure in ^{147}Ce were carried out and agreement with the experimental data is found.

*Electronic address: zhushj@mail.tsinghua.edu.cn

The high-spin states of ^{147}Ce in this work have been studied by measuring coincidence between the prompt γ rays emitted from the spontaneous fission of ^{252}Cf. The experiment was carried out at the Lawrence Berkeley National Laboratory. The Gammasphere detector array consisting of 101 Compton-suppressed Ge detectors was used to detect the γ rays. A γ-γ-γ coincidence matrix (cube) and a γ-γ-γ-γ coincidence matrix (hypercube) were constructed. Detailed information of the experiment can be found in Refs. [13, 14, 23]. The coincidence data were analyzed with the Radware software package using the triple- and four-fold γ coincidence methods [24].

A partial level scheme of ^{147}Ce obtained from the present work is shown in Fig. 1. Three bands are labeled on top of the bands with numbers (1) - (3). Band (1) was observed up to a 2876 keV level in Ref. [20–22]. We confirmed these levels and transitions in this band and significantly expanded it. Three levels at 3472, 3956 and 4552 keV along with three transitions of 596.1, 483.5 and 595.8 keV are added to this band. The 3472 keV level and the 596 keV transition were reported in Ref. [20], but they were not assigned as the members of band (1). Here we assign them as its members. For the side band (2), some levels and transitions were reported in Refs. [20, 22]. In the present work, this band is expanded. Three levels at 1369, 2195 and 2703 keV reported in Refs. [20, 22] are confirmed in this work. The 1742 and 3356 keV levels reported in Ref. [20] as well as the 2610 keV level reported in Ref. [22] are not confirmed in this work. All the other levels and transitions in band (2) are newly identified in this work. The side band (3) is newly established. In addition, several linking transitions between these bands are also identified as shown in Fig 1. As examples, Fig. 2 shows two coincidence γ-ray spectra in ^{147}Ce. In Fig. 2(a), by double gating on the 283.5 and

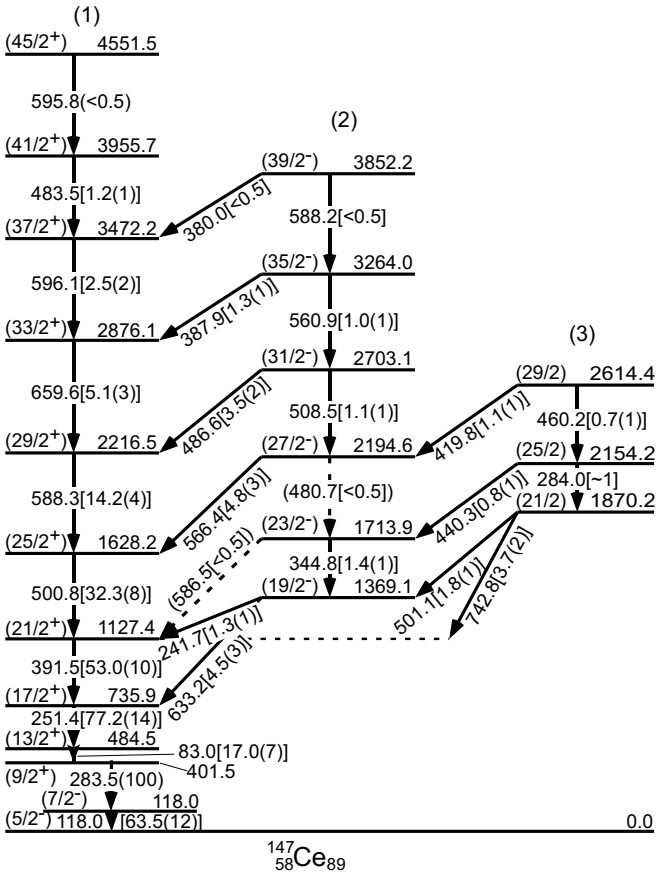

FIG. 1: Partial level scheme of ^{147}Ce identified in the present work. The relative transition intensities and errors are given in square brackets.

251.4 keV γ transitions, all the transitions in Fig. 1 can be seen, except for the 283.5 and 251.4 keV gating γ transitions. Figure 2 (b) is generated by triple gates on the 283.5, 251.4 and 633.2 keV γ transitions. From this figure, one can see the corresponding coincidence γ peaks of 344.8 and tentatively 480.7 keV in band (2), 284.0 and 460.2 keV in band (3), and 501.1 and 440.3 keV between bands (2) and (3). As the intensity of the 480.7 keV transition is weak, the corresponding γ peaks above the 2194.6 keV level can not be seen in this spectrum. However, from Fig. 2(a), one can see these γ peaks. In these spectra, one can see some partner γ transitions in ^{103}Zr (2n), ^{102}Zr (3n), ^{101}Zr (4n), and ^{100}Zr (5n), in addition to the γ peaks observed in ^{147}Ce.

The spin and parity (I^π) of the ground state in ^{147}Ce were tentatively assigned as $5/2^-$. Band (1) was tentatively assigned as positive-parity band with band-head level at 402 keV ($9/2^+$) in Refs. [20, 21] and 485 keV ($13/2^+$) in Ref. [22], respectively. Based on systematical comparison with the $N = 89$ neighboring isotones ^{145}Ba [19] and ^{149}Nd [20], we agree with the 402 keV level assignment, that is, band (1) is built on the 401.5 keV ($9/2^+$) level. It is proposed to arise from the $\nu i_{13/2}$ shell [20]. Several levels in band (2) observed in Ref. [20] were proposed with negative parity. We agree with that assignment. Also based on comparison with the ^{145}Ba [16, 19] and ^{149}Nd [20], band (2) in ^{147}Ce is tentatively assigned as negative-parity band. Thus, in ^{147}Ce, a set of positive- and negative-parity bands (1) and (2) with $\Delta I = 2$ transitions in each band and with linking $E1$ transitions between the two bands form an octupole band structure with a simplex quantum number $s = +i$. It is difficult to assign the I^π's for the band (3) in Fig. 1. We only tentatively assign some spins for band (3), as shown in Fig. 1.

TABLE I: Calculated $B(E1)/B(E2)$ branching ratios in ^{147}Ce.

E_γ (keV)	$I_i^\pi \rightarrow I_f^\pi$	I_γ	$\frac{B(E1)}{B(E2)}$ ($10^{-6}\cdot fm^{-2}$)
486.6	$31/2^- \rightarrow 29/2^+$	3.5(2)	0.72(8)
508.5	$31/2^- \rightarrow 27/2^-$	1.1(1)	
387.9	$35/2^- \rightarrow 33/2^+$	1.3(1)	0.95(12)
560.9	$35/2^- \rightarrow 31/2^-$	1.0(1)	

Now we mainly discuss the characteristics of the octupole correlations in ^{147}Ce. By making systematic comparison of the levels of the $s = +i$ octupole band structures in $N = 89$ odd-A isotones ^{145}Ba [16, 19], ^{147}Ce (in the present work) and ^{149}Nd [20], one can see that they exhibit very similar level energies.

In an octupole band structure, the $B(E1)/B(E2)$ branching ratios can be deduced by using the relation in Ref [12, 13]. The calculated values for ^{147}Ce in the present work are given in Table I. The average $B(E1)/B(E2)$ value for $s = +i$ octupole structure in ^{147}Ce is $0.84\times(10^{-6}\cdot fm^{-2})$, while in the $s = +1$ octupole structures of the even-even Ce isotopes, the average values are 6.12 in ^{144}Ce [10], 1.70 in ^{146}Ce [11], 0.82 in ^{148}Ce [12], 0.04 in ^{150}Ce [13], and $0.023\times(10^{-6}\cdot fm^{-2})$ in ^{152}Ce [14]. The observed $B(E1)/B(E2)$ average value in ^{147}Ce lies between ^{146}Ce and ^{148}Ce, and shows rather stronger octupole correlations, consistent with the systematics.

The energy differences δE between the positive- and negative-parity bands in an octupole band structure can be used to discuss the octupole deformation stability with spin variation. Such δE values can be deduced from the experimental level energies by using the relation [12]:

$$\delta E(I) = E(I^-) - \frac{(I+1)E(I-1)^+ + IE(I+1)^+}{2I+1} \quad (1)$$

Here the superscripts indicate the parities of the levels. Fig. 3 systematically shows plots of the $\delta E(I)$ versus I of the $s = +i$ octupole band structures in $N = 89$ odd-A ^{145}Ba (Z=56) [16, 19], ^{147}Ce (Z=58) and ^{149}Nd (Z=60) [20]. In the limit of stable octupole deformation, $\delta E(I)$ should be close to zero. As seen in Fig. 3, the $\delta E(I)$ decreases with the spin increasing in each isotone. It is close to the stable point at $I \sim 35/2\ \hbar$ for ^{145}Ba. However, for ^{147}Ce and ^{149}Nd, they do not quite reach the stable point at this spin. On the other hand, at the

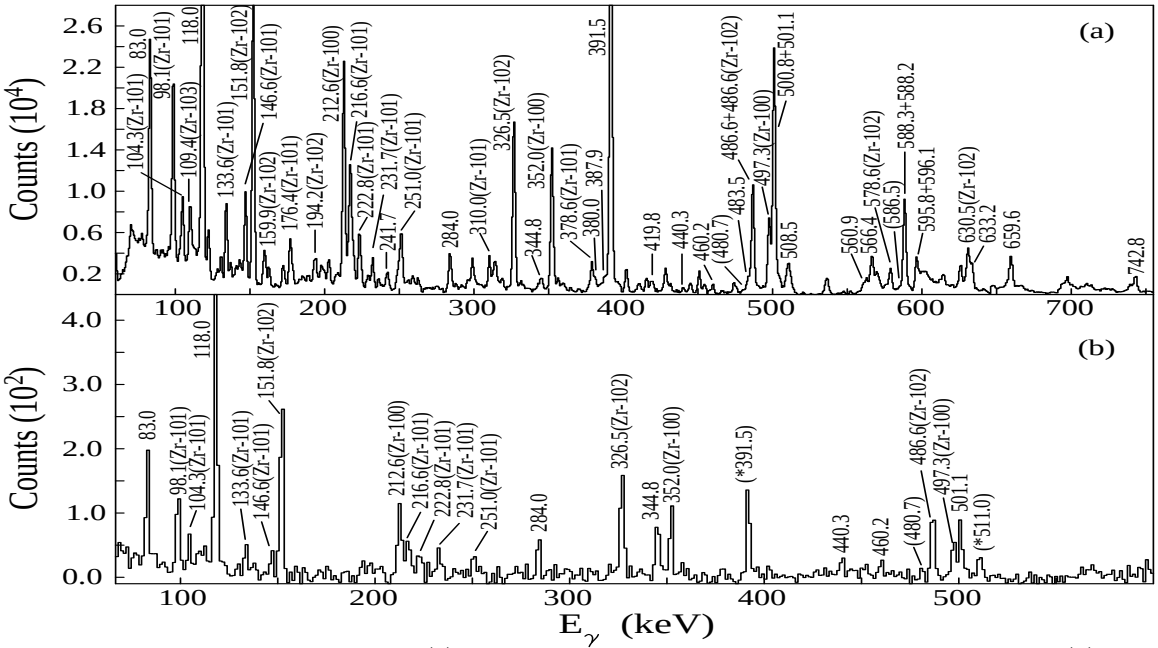

FIG. 2: Portion of the γ-ray spectra obtained by (a) double gating on 283.5 and 251.4 keV γ transitions, and (b) by triple gates on 283.5, 251.4 and 633.2 keV γ transitions in ^{147}Ce. (The 391.5 keV γ peak labeled with (*391.5) comes from the coincidence of the 630.5 keV γ transition in ^{102}Zr partner which is mixed with the 633.2 keV γ transition. The 511.0 keV γ peak labeled with (*511.0) is caused by the annihilation of electrons and positrons).

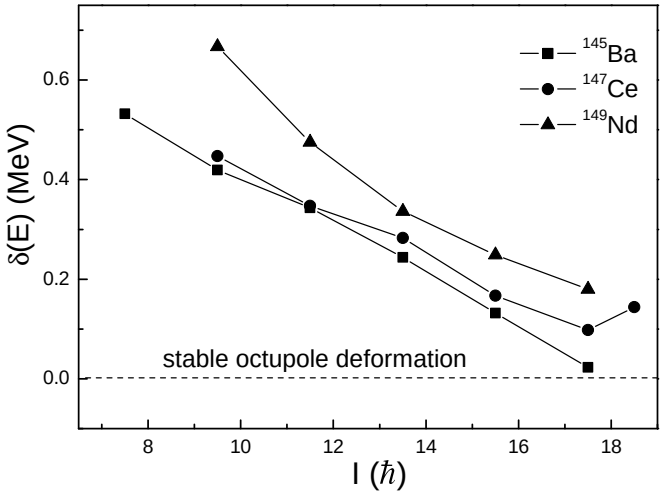

FIG. 3: The systematic comparisons for $\delta E(I)$ versus spin I in ^{145}Ba, ^{147}Ce and ^{149}Nd.

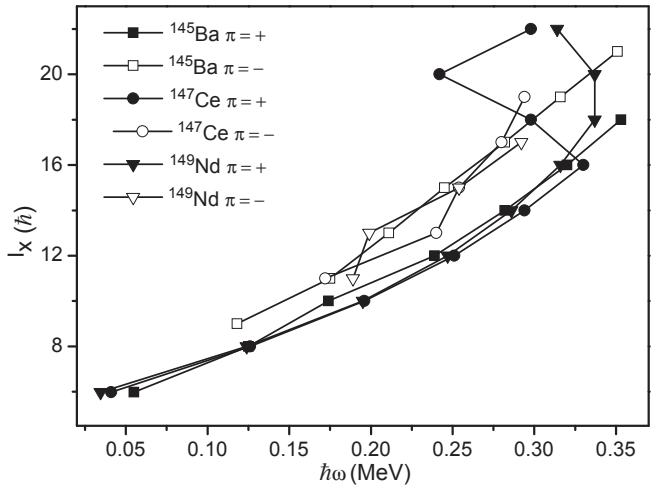

FIG. 4: Plots of the experimental total angular momentum alignment I_x as a function of the rotational frequency for the positive- and negative-parity bands of the $s = +i$ octupole band structures in ^{145}Ba, ^{147}Ce and ^{149}Nd.

same spin value, the $\delta E(I)$ value is least for ^{145}Ba, intermediate for ^{147}Ce and largest for ^{149}Nd. This result shows that the octupole correlations become more unstable as the proton number increases in these $N = 89$ isotones. On the other hand, in ^{147}Ce, as I increases to 39/2 $\hbar$, $\delta E(I)$ increases, and the octupole correlations become more unstable than that at 37/2 $\hbar$. This up-turn is likely related to the backbending of I_x above the 2876.1 keV level seen in Fig. 4.

Fig. 4 shows the total angular momentum alignment I_x vs. the rotational frequency $\hbar\omega$ in positive- and negative-parity bands of the $s = +i$ octupole band structures in $N = 89$ odd-A ^{145}Ba (Z=56) [16, 19], ^{147}Ce (Z=58) and ^{149}Nd (Z=60) [20], where $I_x = \sqrt{(I_a + 1/2)^2 - K^2)}$, $I_a = (I_i + I_f)/2$, $\hbar\omega = (E_i - E_f)/[I_x(I_i) - I_x(I_f)]$, with proposed $K = 1/2$ (see the later RASM calculations). One can see that the I_x values are very close to each other in those $N = 89$ isotones. On the other hand, the I_x value in the negative-parity bands is larger than those in the positive parity bands in each isotone, which is also

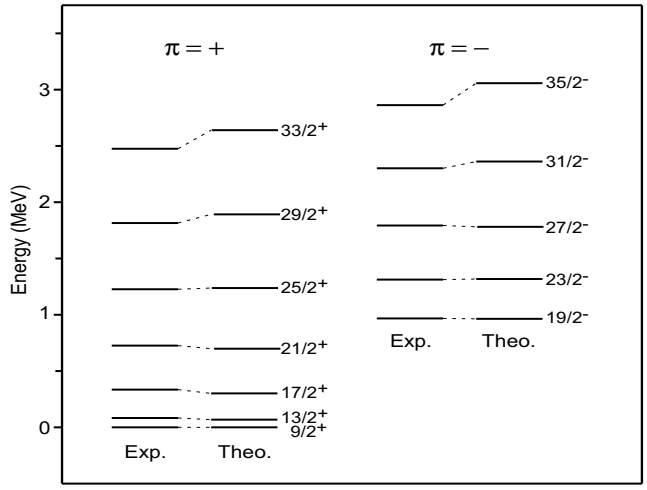

FIG. 5: Comparison of the calculated energy levels for ^{147}Ce with experimental data. The energies of the $9/2^+$ states have been taken as a reference.

observed in $s = +1$ octupole bands in even-even Ce isotopes [14]. On the other hand, one can also see that in the positive-parity band (1) the backbendings occur at $\hbar\omega \sim 0.29$ MeV for ^{147}Ce and $\hbar\omega \sim 0.33$ MeV for ^{149}Nd. These backbendings are likely caused by the alignment of a pair of $h_{11/2}$ protons, because the backbendings corresponding to the alignment of neutrons should be blocked by the odd neutron.

In order to understand the characteristics of the octupole correlations in ^{147}Ce, we have carried out RASM calculations. This model was first developed to describe octupole deformation of the even-even Ra isotopes in the $A = 220$ region [25]. Then it was successfully adapted to describe the octupole deformation and octupole correlations in the $Z = 56$, $N = 88$ region, for example, in some Ce and Ba isotopes [11, 26, 27]. The details about RASM can be found in Refs. [25–27]. For ^{147}Ce, the deformation parameters used in the calculations are as follows: $\varepsilon_2 = 0.173$, $\varepsilon_3 = 0.082$ and $\varepsilon_4 =$ -0.04, which are close to the values presented in Ref. [28]. The calculations indicate that the ground state in ^{147}Ce originates from the $\nu f_{7/2}$ mixed with $\nu h_{9/2}$ configurations. For the $s = +i$ octupole band structure in ^{147}Ce, the results of our calculations and comparison with the experimental data are shown in Fig. 5. One can see that until medium spin states are reached, the excitation energies of levels of ^{147}Ce are well reproduced by the RASM calculations. The calculations show that the $s = +i$ octupole band structure originates from the $i_{13/2}$ [660]1/2 orbital with $K = 1/2$. The calculated results give another evidence for octupole correlations in ^{147}Ce.

The characteristics for the weak band (3) in ^{147}Ce are not clear, and more work is needed to understand it.

In summary, the high-spin structure of neutron-rich ^{147}Ce has been reinvestigated. The previously observed band structures have been expanded and a third new band added. An octupole band structure based on the $i_{13/2}$ orbital has been proposed. Observed $B(E1)/B(E2)$ branching ratios indicate that the octupole correlations in ^{147}Ce are rather strong. The reflection asymmetric shell model calculations for the octupole band structure of ^{147}Ce are in good agreement with the experimental data. Other characteristics of octupole band structures are systematically discussed.

The work at Tsinghua University, China Institute of Atomic Energy was supported by the National Natural Science Foundation of China under Grants No. 11175095, 11275067, 11205246. The work at Vanderbilt University, Lawrence Berkeley National Laboratory was supported, respectively, by U. S. Department of Energy under Grant and Contract No. DE-FG05-88ER40407, DE-AC03-76SF00098.

[1] W. Nazarewicz *et al.*, Nucl. Phys. A **429**, 269 (1984).
[2] W. Nazarewicz and S. L. Tabor, Phys. Rev. **C 45**, 2226 (1992).
[3] P. A. Butler and W. Nazarewicz, Rev. Mod. Phys. **68**, 349 (1996).
[4] J. H. Hamilton *et al.*, Prog. Part. Nucl. Phys. **35**, 635 (1995).
[5] W. R. Phillips *et al.*, Phys. Rev. Lett. **57**, 3257 (1986).
[6] S. J. Zhu *et al.*, Phys. Lett. B **357**, 273 (1995).
[7] W. Urban *et al.*, Nucl. Phys. A **613**, 107 (1997).
[8] S. J. Zhu *et al.*, Chin. Phys. Lett. **14**, 569 (1997).
[9] W. R. Phillips *et al.*, Phys. Lett. B **212**, 402 (1988).
[10] L. Y. Zhu *et al.*, High Energy Phys. and Nucl. Phys.-Chinese Edition **22**, 885 (1998).
[11] Y. J. Chen *et al.*, High Energy Phys. and Nucl. Phys.-Chinese Edition **30**, 740 (2006).
[12] Y. J. Chen *et al.* Phys. Rev. C **73**, 054316 (2006).
[13] S. J. Zhu *et al.*, Phys. Rev. C **85**, 014330 (2012).
[14] H. J. Li *et al.*, Phys. Rev. C **86**, 067302 (2012).
[15] Y. X. Luo *et al.*, Nucl. Phys. A **838**, 1 (2010).
[16] S. J. Zhu *et al.*, Phys. Rev. C **60**, 051304 (1999).
[17] S. J. Zhu *et al.*, Phys. Rev. C **59**, 1316 (1999).
[18] Ts. Venkova *et al.*, Eur. Phys. J. A **26**, 315 (2005).
[19] T. Rząca-Urban *et al.*, Phys. Rev. C **86**, 044324 (2012).
[20] Ts. Venkova *et al.*, Eur. Phys. J. A **28**, 147 (2006).
[21] F. Hoellinger *et al.*, Phys. Rev. C **56**, 1296 (1997).
[22] M. Sakhaee *et al.*, Phys. Rev. C **60**, 067303 (1999).
[23] H. J. Li *et al.*, Phys. Rev. C **88**, 054311 (2013).
[24] D. C. Radford, Nucl. Instrum. Methods Phys. Res. A **361**, 297 (1995).
[25] Y. S. Chen and Z. C. Gao, Phys. Rev. C **63**, 014314 (2000).
[26] Y. J. Chen *et al.*, Chin. Phys. Lett. **22**, 1362 (2005).
[27] Y. J. Chen *et al.*, High Energy Phys. and Nucl. Phys.-Chinese Edition **32**, Suppl. II, 158 (2008).
[28] P. Möller *et al.*, At. Data and Nuc. Data Tab. **94**, 758 (2008).